

# Simulations of metastable states near the apex of a force microscope tip interacting with an ionic crystalline surface

B. Ittermann,<sup>1</sup> R. Hoffmann-Vogel,<sup>1,\*</sup> L. Behrens,<sup>1</sup> and A. Baratoff<sup>2</sup>

<sup>1</sup>*Physikalisches Institut and Deutsche Forschungsgemeinschaft Center for Functional Nanostructures, Karlsruhe Institute of Technology Campus South, D-76128 Karlsruhe, Germany*

<sup>2</sup>*National Center of Competence in Research on Nanoscale Science, Institute of Physics, University of Basel, Klingelbergstrasse 82, CH-4056 Basel, Switzerland*

(Received 13 August 2012; revised manuscript received 2 May 2013; published 22 May 2013)

Atoms or pairs of ions picked up by probe tips used in dynamic force microscopy (DFM) can be strongly displaced and even hop discontinuously upon approach to the sample surface. The energy barriers for some of those hops are of the right order of magnitude to explain the rise in energy dissipation commonly observed in DFM measurements at room temperature. The systematic computations reported here can explain the infrequent jumps and very low average energy dissipation observed at low temperature in a previous DFM study on a KBr(001) sample. Close to the surface we indeed find new states separated by small energy barriers which account for those phenomena. These energy barriers strongly depend on details of the atomic arrangement in the vicinity of the tip apex.

DOI: [10.1103/PhysRevB.87.195437](https://doi.org/10.1103/PhysRevB.87.195437)

PACS number(s): 07.79.Lh, 61.46.-w, 34.20.Cf, 68.35.-p

## I. INTRODUCTION

Dynamic force microscopy (DFM) has developed into a valuable tool not only for surface characterization of nonconducting samples but also for controlled modification at the atomic level. This has become possible mainly thanks to sensitive measurement modes in which the tip is oscillated with a constant amplitude in the nm range at a resonance frequency of the force sensor.<sup>1</sup> Atomic-scale precision is then achieved if the tip apex stays or periodically comes to distances at which short-range site-selective forces act, thereby causing a measurable frequency shift. Atom manipulation experiments in that mode have inspired computations of changes in the potential landscape induced by the tip apex and of resulting fingerprints in measurable quantities on semiconductor surfaces,<sup>2-5</sup> as well as on ionic crystal surfaces.<sup>6,7</sup> The average dissipation of energy stored in the cantilever oscillation also exhibits atomic-scale contrast, even on defect-free surfaces, and its magnitude indicates that it mainly originates from hysteretic hopping of atoms between two or more stable positions.<sup>8,9</sup> Sudden but infrequent contrast changes, typically more pronounced in dissipation images, have been attributed to long-lived rearrangements of the tip apex.<sup>10</sup> A reproducible change in the tip polarity when the tip is moved across a KBr substrate step has also been attributed to the rearrangement of a small number of atoms on the tip apex.<sup>11</sup>

Three different causes of dissipation induced by hysteretic tip-sample interactions must be considered: hopping on the sample, hopping between the tip and surface, and hopping on the tip. Hopping on the sample is usually not expected because diffusion or other rearrangements on clean flat terraces of low-index surfaces usually involve rather high-energy barriers, except for some reconstructed surfaces which exhibit bistable configurations.<sup>12</sup> The presence of long-lived localized defects can be excluded by taking high-resolution images. However, in scanning tunneling microscopy studies,<sup>13</sup> as well as for DFM on insulating surfaces, mobile adsorbates can merely lead to blurry or streaky images and to additional noise in a certain temperature range, thus causing blurred or streaky images

when the scan and hopping rates roughly match.<sup>14</sup> Hopping between the tip and sample,<sup>8,9</sup> which can in the extreme case even lead to atomic chain formation and breaking in some oscillation cycles,<sup>15</sup> manifests itself indirectly via the average energy dissipation. However, in order to unambiguously interpret measured results, the third scenario, hopping on the tip, must be considered.<sup>16,17</sup> This is in general difficult because the structure and chemical composition of the tip are unknown. For many commonly studied crystals (Si, KBr, and NaCl), there are indications that sample material is picked up by the tip owing to intentional or accidental contact prior to or during DFM measurements. Using large-scale simulations several groups have characterized force microscope tips and derived construction principles for realistic model tips from comparisons with experiments.<sup>4,7,15</sup>

## II. MODEL TIP

Here, we study possible low-energy configurations of an overall neutral KBr tip supporting two additional ions and its interaction with a KBr (001) surface by means of extensive computations. The employed code, based on an atomistic shell model, was developed for simulations of DFM on ionic crystals<sup>10,18</sup> and validated in previous studies.<sup>19,20</sup> Such a model tip may represent the end of a nominal silicon tip typically used in force microscopy experiments decorated by sample material. More precisely, our model tip consists of a K<sup>+</sup> terminated cubic cluster of 64 K (ionic radius 152 pm) and Br (ionic radius 182 pm) ions exposing stable {001} facets oriented such that the (111) direction is perpendicular to the sample surface. One K<sup>+</sup> and one Br<sup>-</sup> ion are added near one of the ⟨100⟩ edges meeting at the tip apex, using their bulk separation of 326.4 pm, and then allowed to relax, as illustrated in Fig. 1 (right) (values are taken from Ref. 21.). The initial configuration of these two additional ions is chosen in accordance with simulations and a previous experimental study of diffusion on surfaces of rocksalt-type crystals.<sup>22</sup> This model is well

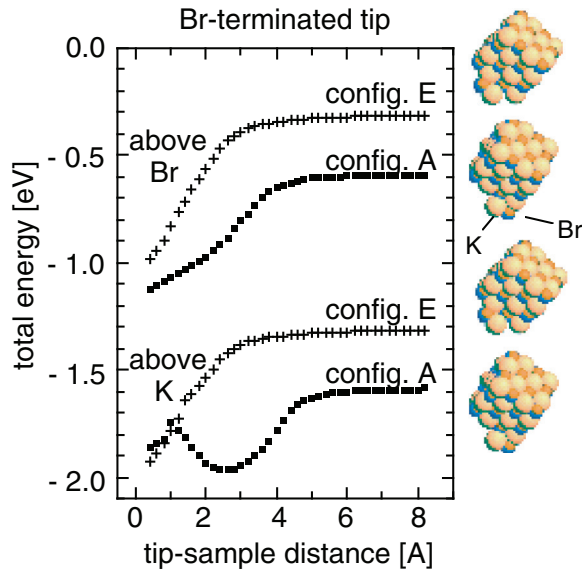


FIG. 1. (Color online) Interaction energy with respect to an arbitrary offset chosen for visual clarity as a function of decreasing nominal tip-sample distance for the  $\text{Br}^-$  terminated tip in configurations A and E illustrated on the right. In both cases the rigid top half of the tip is approached along the same path such that the protruding  $\text{Br}^-$  in configuration A is initially above a  $\text{Br}^-$  or a  $\text{K}^+$  surface ion. The data calculated above  $\text{K}^+$  are offset by  $-1$  eV for clarity.

suit for studying rearrangements of the simplest moiety likely to be picked upon gentle contact with the sample. Alternatively, the supported KBr dimer may be the remnant of a broken chain of ions formed during tip retraction.<sup>15,23</sup> The assumed tip configuration is probably more likely than alternative ones involving other kinds of defects which produce appreciable force hysteresis and energy dissipation in the case of chemically similar NaCl model tips.<sup>7</sup> The sample was represented by a slab containing six layers of  $10 \times 10$  ions each. Although in previous calculations, additionally to the atomistic part of the tip, the macroscopic body of the tip was represented by a conductive sphere,<sup>10,18</sup> in the calculations shown here only the interaction between ions was considered. This assumption considerably reduces the required computational time and has been recently justified for overall charge neutral tip and sample subsystems.<sup>24</sup> These interactions are calculated from pairwise Buckingham and Coulomb potentials at zero temperature with the exception of the first movie in the supporting information. Ions are treated in a shell model with independently relaxed positions of coupled shells and cores with parameters taken from Ref. 21. The interaction of the tip with the sample was computed with all ions in the topmost half of the tip as well as the bottom layer of the sample and the sides fixed. More details about the simulation procedure can be found in previous publications.<sup>19,20</sup>

First, the properties of the decorated tip alone were studied. One stable and four metastable configurations labeled A to E were found by constrained minimization while shifting the additional  $\text{Br}^-$  ion parallel to the edge (projected reaction coordinate  $q$ ) and letting its two orthogonal coordinates and those of all ions in the bottom half of the cube relax. The

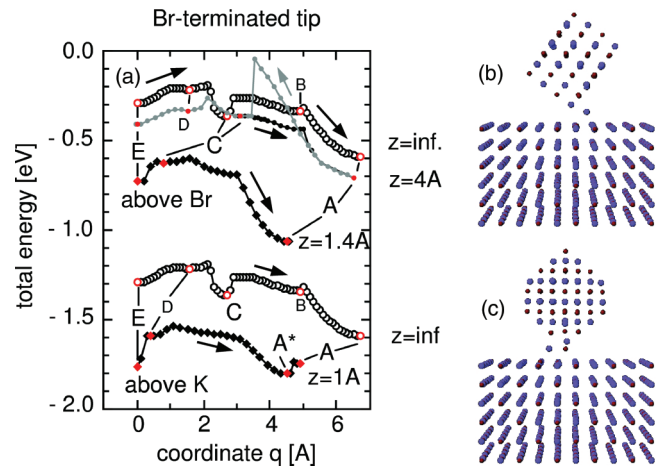


FIG. 2. (Color online) (a) Interaction energy profiles calculated for the initially protruding  $\text{Br}^-$  tip ion above equally and oppositely charged surface ions at a few nominal tip-sample distances. The coordinate  $q$  axis of the moved  $\text{Br}^-$  is aligned with the cube edge pointing toward the cube apex. The data above  $\text{K}^+$  have been offset by  $-1$  eV for clarity. All black curves represent constrained minimizations at  $q$  increments of  $0.1$  Å. The red points refer to subsequent full minimizations. (b and c) Side views on the new configuration  $A^*$ , viewed along the  $x$  and  $y$  directions, respectively.

corresponding profiles labeled  $z = \text{inf}$  are shown in Fig. 2. In configurations A and E, the additional  $\text{Br}^-$  and  $\text{K}^+$  ions are essentially located along the cube edge, and the positions of the  $\text{Br}^-$  ion differ between both configurations by approximately one bulk lattice constant. The lowest total energy was found for ( $\text{Br}^-$  terminated) configuration A, because the electrostatic field outside the cube is enhanced in the vicinity of the low-coordinated edge, especially around the apex. For the same reason the energy barrier to reach configuration A starting from E is much lower than for the opposite process. Configurations B and D arise when the additional  $\text{Br}^-$  ion is located above a bridge site on one facet adjacent to the cube edge. Between  $q = 2.1$  and  $2.9$  Å the initial  $\text{Br}^-$  ion dips into the cubic cluster while a nearby bromine ion emerges from the cluster to form configuration C. Ion exchange processes analogous to that just described were also found in previous simulations of an MgO dimer diffusing on the MgO (001) surface.<sup>25</sup> Similar configurations were found when all  $\text{Br}^-$  ions were replaced by  $\text{K}^+$  ions and vice versa.

To test the thermal stability of the different tip configurations, molecular-dynamics simulations were performed at  $T = 200, 300,$  and  $500$  K for the  $\text{K}^+$  and the  $\text{Br}^-$  terminated tip in configuration A. Below  $500$  K, no hopping was observed over the relatively short simulation time. At  $T = 500$  K the former tip showed a transition from the E to the A configuration nicely visualized in a movie.<sup>26</sup> In this transition the  $\text{K}^+$  ion did not, however, jump directly to the final position. Instead, it moved to the position of a nearby  $\text{K}^+$  ion in a configuration similar to that called C in the constrained minimizations mentioned earlier. This exchanged  $\text{K}^+$  ion then moved to the position of the  $\text{K}^+$  ion in the A configuration. Such exchange processes compete against pivoting around the dimer partner as in diffusion on (001) surfaces<sup>22,25</sup> and may even be favored in the present lower coordination situation.

### III. APPROACH TO THE SURFACE: NEW CONFIGURATIONS

In a second step, the interaction of the tip with the sample surface and possible hysteretic processes were studied as a function of the nominal tip-sample distance defined as the separation of the foremost ions when ignoring relaxation. Ions in the top half of the tip cluster and in two boundary layers of the sample slab were frozen, while the rest were allowed to relax. The rigid part of the tip was incrementally approached perpendicular to the surface such that the protruding  $\text{Br}^-$  in configuration *A* was facing a particular surface ion. The results were compared to configuration *E* at the same positions of the rigid tip body (Fig. 1). If the tip is approached above an ion of the same charge, the energy difference between configurations *A* and *E* becomes smaller, but never vanishes. In contrast, if the tip is approached above an oppositely charged ion, the energy first drops faster and then the energy difference decreases and vanishes for the  $\text{K}^+$  terminated tip and even becomes negative for the  $\text{Br}^-$  terminated tip below a critical tip-sample distance of about 1 Å. One therefore expects the  $\text{Br}^-$  terminated tip to change from configuration *A* to configuration *E* below that distance if the energy barrier between the two states can be overcome by thermal fluctuations.

In order to investigate changes in the energy landscape induced by the tip approach, we performed constrained minimizations like those discussed in Sec. II at a few tip-sample distances. Figure 2 shows that the number and character of the metastable configurations changes significantly. While at relatively large distances five configurations analogous to *A–E* are observed, only three remain at close tip-sample distances above the  $\text{Br}^-$  surface ion. Lateral hysteresis is also observed, e.g., for  $z = 1$  Å, indicating the presence of inequivalent energy barriers along paths starting from configurations *A* and *E*. A new configuration (*A\**), even lower in energy than configuration *A*, appears above the oppositely charged  $\text{K}^+$  surface ion for  $z = 1$  Å. In configuration *A\** the additional  $\text{K}^+$  and  $\text{Br}^-$  ions of the molecule are bound to both the tip and surface. This configuration arises when the body of the cubic tip pushes the added dimer aside, until the dimer ions approximately bind to ions of opposite charge on the surface as well as on a tip facet, as illustrated in another set of movies.<sup>27</sup>

### IV. ENERGY BARRIERS FOR CONFIGURATIONAL CHANGES

Our study originally focused on hopping between *A* and *E* configurations, because simulations of diffusion on rocksalt type (001) surfaces identified this process as the most probable.<sup>22</sup> The presence of intermediate metastable configurations implies that direct hopping between *A* and *E* is less probable than hopping via the intermediate states *B–D*, due to the reduced intervening energy barriers, which are the relevant ones for thermal activation. The energy barriers are summarized in Table I. The highest-energy barrier between any of those configurations represents the bottleneck of the process and therefore determines the effective hopping rate. The bottleneck barrier for the transition from *E* to *A* ranges from 80 to 175 meV, while the bottleneck barrier for the opposite

TABLE I. Summary of all the energy barriers obtained in constrained minimizations above different surface sites.

Surface site	Tip-sample distance (Å)	Transition path	Energy barrier (meV)	Bottleneck	
–	$\infty$	<i>A</i> → <i>B</i>	272	×	
		<i>B</i> → <i>C</i>	78		
		<i>C</i> → <i>D</i>	176		
		<i>D</i> → <i>E</i>	7		
Br	4.0	<i>A</i> → <i>C</i>	662	×	
		<i>C</i> → <i>D</i>	94		
		<i>D</i> → <i>E</i>	4		
	1.4	<i>A</i> → <i>C</i>	461	×	
		<i>C</i> → <i>E</i>	3		
K	1.0	<i>A</i> → <i>A*</i>	10	×	
		<i>A*</i> → <i>D</i>	264		
		<i>D</i> → <i>E</i>	2		
–	$\infty$	<i>E</i> → <i>D</i>	88	×	
		<i>D</i> → <i>C</i>	25		
		<i>C</i> → <i>B</i>	103		
		<i>B</i> → <i>A</i>	23		
	Br	4.0	<i>E</i> → <i>D</i>	83	×
			<i>D</i> → <i>C</i>	67	
			<i>C</i> → <i>A</i>	0.1	
		1.4	<i>E</i> → <i>C</i>	107	×
<i>C</i> → <i>A</i>	22				
K	1.0	<i>E</i> → <i>D</i>	174	×	
		<i>D</i> → <i>A*</i>	51		
		<i>A*</i> → <i>A</i>	64		

transition from *A* to *E* ranges from 260 to 660 meV for all of the constrained energy profiles studied.<sup>28</sup> These values should be compared to the thermal energy at room temperature (25 meV) or at low temperatures (8–40 K,<sup>16</sup> i.e., 0.7–3.4 meV) depending on the experiment to be considered. Two limiting cases are of particular interest:<sup>16,17</sup> if the hopping rate is low enough (one jump every 0.1–10 s), individual atomic jumps can be experimentally observed. If, in contrast, the hopping rate exceeds the cantilever oscillation frequency ( $\sim 100$ – $200$  kHz) the individual states involved are averaged over in a dynamic force measurement, but the energy dissipation due to hops into lower-energy configurations becomes appreciable. Our results imply that, for most potential-energy landscapes so far considered, the tip configuration would be rapidly flipping at room temperature on time scales faster than the cantilever oscillation, but tip changes due to hops would be frozen out at low temperatures. The main reason is that in configuration *A* the protruding  $\text{Br}^-$  ion is subjected to the positive electrostatic potential localized around the apex of the cube.<sup>29</sup> This lowers its interaction energy in configuration *A* and thus raises the bottleneck energy barrier between *A* and *E*. Therefore, hopping between *A* and *E* can only account for weak energy dissipation at room temperature but not for the distinct single jumps observed at low temperatures.<sup>16</sup>

As an alternative model tip one may consider a KBr cubic cluster with the additional  $\text{K}^+$  and  $\text{Br}^-$  ions placed in positions of higher coordination, such as a facet. However, with this

premise it is more difficult to realize an atomically sharp tip, as required for lattice-resolved images without appreciable distortions<sup>30</sup> observed experimentally.

## V. LOW-ENERGY BARRIERS

The jumps observed at low temperatures might be explained by the occurrence of new states similar to  $A^*$ . Indeed, the energy barrier between  $A$  and  $A^*$  being only 64 meV at a tip-sample distance of 1 Å, individual jumps could be observed at temperatures between 25 and 30 K.

In order to investigate the latter possibility in more detail, we calculated the total energy as a function of tip-sample distance for inequivalent rotations of the  $\text{Br}^-$  terminated tip around the  $z$  axis perpendicular to the sample surface passing through a surface  $\text{K}^+$  site. The relative orientation of the tip and sample is shown schematically in Fig. 3(d) viewed from above. We define  $0^\circ$  as the rotation angle at which the added  $\text{KBr}$  dimer is aligned with one of the  $\langle 100 \rangle$  axes of the sample. In this notation our previous calculations correspond to  $30^\circ$ . Due to the symmetries of the surface and the model tip, full information is contained for polar angles between  $0$  and  $45^\circ$ . First, the tip rotation was adjusted at large tip-sample distances. Then the interaction energy of the tip and surface was calculated as a function of tip-sample distance while

the tip was approached to the surface. At distances larger than about 2.0 Å, the data are qualitatively and quantitatively similar for all rotation angles [Figs. 3(a) and 3(b)]. However, at smaller distances significant differences occur. Between  $30$  and  $45^\circ$ , a jump in the energy arises at an angle-dependent critical distance below the interaction energy minimum. At smaller distances, the interaction energy decreases again upon approach. This behavior can be identified with state  $A^*$  discussed above, as evident in movies of the approach.<sup>27</sup> In contrast, between  $0$  and  $20^\circ$ , the energy continuously increases further upon approach in the same distance regime. The foremost tip ion then remains in a deformed state  $A$  roughly under the tip apex, while for angles between  $30$  and  $45^\circ$  the foremost tip atom jumps toward a next-neighbor surface ion of opposite sign while the dimer becomes aligned with a surface  $\langle 100 \rangle$  direction, as well as with a tip facet in configuration  $A^*$ . For  $20^\circ$  the energy versus distance curve is deformed around the critical distance, an indication of the proximity to an additional state, but the tip remains in the deformed state  $A$ .

We finally studied the stability of configuration  $A^*$ . When the tip is retracted starting from distances larger than critical, the initial values of the energy, force, and atomic positions are smoothly recovered. Otherwise hysteresis is observed until eventually another jump restores the initial energy, force, and atomic positions at a larger tip-sample critical distance. In Fig. 3(c) an example for  $30^\circ$  is shown, which is also further documented in a movie of the simulated retraction.<sup>31</sup> Since our calculations are done at zero temperature, the observed hysteresis implies that the energy barrier between  $A$  and  $A^*$  vanishes at the critical distance of approach and that energy is gained by jumping to  $A^*$  at closer tip-sample distances. Similarly, upon retraction, energy is gained by jumping back to state  $A$  while the reverse energy barrier vanishes at the critical distance of retraction. Between the two critical points a finite-energy barrier exists between the two states. This variation of the energy landscape as a function of tip-sample distance corresponds to the scenario proposed by Sasaki and Tsukada<sup>8</sup> with the modification that the atomic hops themselves need not occur in the  $z$  direction between the tip and the sample but must only be induced by the tip motion perpendicular to the sample surface. Results obtained for different relative orientations of the tip are summarized in Table II. The energy loss in the approach-retraction cycle of the tip is equal to the area enclosed between the two distinct force-distance curves between both critical distances and amounts to up to 0.2 eV, which is in the range of what is expected from low-temperature experiments.<sup>16</sup>

We further characterized the stability of configuration  $A^*$  by studying the energy barrier from state  $A$  to state  $A^*$  in constrained minimizations along the previously defined reaction coordinate  $q$ . The tip-sample distance was chosen to be 0.13 nm because this is the largest distance at which state  $A^*$  is observed during approach and in a finite distance range upon retraction, and so we expected that the state could be observed for several tip angles. Indeed, between  $30$  and  $40^\circ$ , where  $A^*$  was observed in energy versus distance data, state  $A^*$  is also observed in constrained minimizations. For  $20^\circ$ , although state  $A^*$  is not observed during approach, the system can be driven into a similar state under the constraint. The energy barriers range between 19 and 91 meV

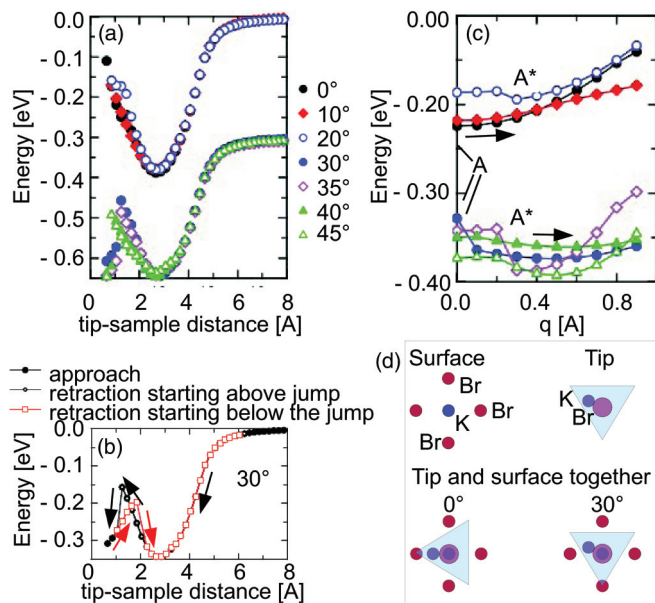


FIG. 3. (Color online) Interaction energy as a function of distance for different polar angles of the  $\text{Br}^-$  terminated tip with respect to the  $[001]$  axis passing through a surface  $\text{K}^+$  site. (a) Between  $0$  and  $20^\circ$  no jump occurs, while between  $30$  and  $45^\circ$  (curves offset by  $-0.3$  eV for clarity) hysteresis is observed in the investigated distance range. (b) Approach-retraction hysteresis observed for  $30^\circ$ . (c) Results of constrained minimizations for orientations where no jump was observed and (curves offset by  $-0.3$  eV for clarity) for those where hysteresis was observed. (d) Schematic drawing illustrating two inequivalent orientations of the tip cluster with the initially on-edge adsorbed dimer with respect to a surface unit cell viewed from above.

TABLE II. Critical distances, hysteresis loop areas, and energy barriers for different tip orientations. To obtain the data, the tip was first approached to the surface up to a distance of 1.3 Å, the dimer was forced into state  $A^*$  by the constraint, the system was fully relaxed, and finally the tip was retracted. For  $20^\circ$  a configuration similar to  $A^*$  is only reached under the constraint, but, upon retraction from this configuration, the two added ions remain on the surface, so that critical distances and hysteresis are not observed.

Rotation angle ( $^\circ$ )	Critical distance of approach (Å)	Critical distance of retraction (Å)	Hysteresis loop area (meV)	Energy barrier $A^* \rightarrow A$ (meV)
20	–	–	–	19
30	1.3	2.1	200	91
35	1.3	2.1	170	93
40	1.1	2.7	190	23
45	0.9	1.9	90	40

depending on the tip orientation. These energy barriers are of the right order of magnitude for explaining the infrequent jumps seen in low-temperature experiments.<sup>16</sup> One should, however, consider that the chosen reaction coordinate  $q$  was not modified to take into account the tip deformation. It is therefore possible that even-lower-energy barriers occur in other directions, in particular at close tip-sample distances. Obviously, the precise values of the energy barriers depend on the details of the atomic arrangement of the tip.

## VI. CONCLUSIONS

We conclude that ion pairs picked by force microscope tips decorated by sample material can be strongly displaced upon approach to the sample surface, in particular at close tip-sample distances, where they become bound to both the tip and sample. The resulting hops have components parallel to the sample surface. Some of those hops can account for rapid flipping of the tip configuration at room temperature. In addition, some metastable states which occur at close tip-sample distances can be separated by energy barriers that are low enough to explain infrequent individual jumps observed at low temperatures. The adsorbed dimers have a tendency to align with ions of opposite charge on the sample surface. Ion exchange processes previously identified in a study of surface diffusion are preferred for some of the investigated hops. Back and forth hops between metastable configurations result in a hysteretic force as a function of distance. The energy dissipated by such hops is in the range of what is expected from low-temperature experiments.<sup>16</sup>

## ACKNOWLEDGMENTS

Financial support from the Landesstiftung Baden-Württemberg in the framework of its excellence program for postdoctoral researchers, from the European Research Council through the Starting Grant NANOCNTACTS (Grant No. 239838) and from the National Center of Competence in Research on Nanoscale Science of the Swiss National Science Foundation, is gratefully acknowledged.

\*r.hoffmann@kit.edu

<sup>1</sup>Noncontact Atomic Force Microscopy, edited by S. Morita, R. Wiesendanger, and E. Meyer (Springer, Berlin, 2002).

<sup>2</sup>L. Pizzagalli and A. Baratoff, *Phys. Rev. B* **68**, 115427 (2003).

<sup>3</sup>P. Dieska, I. Stich, and R. Perez, *Phys. Rev. Lett.* **95**, 126103 (2005).

<sup>4</sup>N. Oyabu, P. Pou, Y. Sugimoto, P. Jelinek, M. Abe, S. Morita, R. Perez, and O. Custance, *Phys. Rev. Lett.* **96**, 106101 (2006).

<sup>5</sup>O. Custance, R. Perez, and S. Morita, *Nature Nanotechnology* **4**, 803 (2009).

<sup>6</sup>T. Trevethan, M. Watkins, L. N. Kantorovich, A. L. Shluger, J. Polesel-Maris, and S. Gauthier, *Nanotechnology* **17**, 5866 (2006).

<sup>7</sup>F. F. Canova and A. S. Foster, *Nanotechnology* **22**, 045702 (2011).

<sup>8</sup>N. Sasaki and M. Tsukada, *Jpn. J. Appl. Phys.* **39**, L1334 (2000).

<sup>9</sup>L. N. Kantorovich and T. Trevethan, *Phys. Rev. Lett.* **93**, 236102 (2004).

<sup>10</sup>R. Bennowitz, A. S. Foster, L. N. Kantorovich, M. Bammerlin, C. Loppacher, S. Schär, M. Guggisberg, E. Meyer, and A. L. Shluger, *Phys. Rev. B* **62**, 2074 (2000).

<sup>11</sup>M. A. Venegas de la Cerda, J. Abad, A. Madgavkar, D. Martrou, and S. Gauthier, *Nanotechnology* **19**, 045503 (2008).

<sup>12</sup>L. N. Kantorovich and C. Hobbs, *Phys. Rev. B* **73**, 245420 (2006).

<sup>13</sup>J. C. Dunphy, P. Sautet, D. F. Ogletree, O. Dabbousi, and M. B. Salmeron, *Phys. Rev. B* **47**, 2320 (1993).

<sup>14</sup>M. Watkins, T. Trevethan, A. L. Shluger, and L. N. Kantorovich, *Phys. Rev. B* **76**, 245421 (2007).

<sup>15</sup>S. Kawai, F. F. Canova, T. Glatzel, A. S. Foster, and E. Meyer, *Phys. Rev. B* **84**, 115415 (2011).

<sup>16</sup>R. Hoffmann, A. Baratoff, H. J. Hug, H. R. Hidber, H. v. Löhneysen, and H.-J. Güntherodt, *Nanotechnology* **18**, 395503 (2007).

<sup>17</sup>S. A. Ghasemi, S. Goedecker, A. Baratoff, T. Lenosky, E. Meyer, and H. J. Hug, *Phys. Rev. Lett.* **100**, 236106 (2008).

<sup>18</sup>L. N. Kantorovich, A. S. Foster, A. L. Shluger, and A. M. Stoneham, *Surf. Sci.* **445**, 283 (2000).

<sup>19</sup>R. Hoffmann, L. N. Kantorovich, A. Baratoff, H. J. Hug, and H.-J. Güntherodt, *Phys. Rev. Lett.* **92**, 146103 (2004).

<sup>20</sup>K. Ruschmeier, A. Schirmeisen, and R. Hoffmann, *Phys. Rev. Lett.* **101**, 156102 (2008).

<sup>21</sup>M. J. L. Sangster and R. M. Atwood, *J. Phys. C* **11**, 1541 (1978).

<sup>22</sup>A. L. Shluger, A. L. Rohl, and D. H. Gay, *Phys. Rev. B* **51**, 13631 (1995).

<sup>23</sup>M. A. Lantz, R. Hoffmann, A. S. Foster, A. Baratoff, H. J. Hug, H. R. Hidber, and H.-J. Güntherodt, *Phys. Rev. B* **74**, 245426 (2006).

<sup>24</sup>A. Sadeghi, A. Baratoff, S. A. Ghasemi, S. Goedecker, T. Glatzel, S. Kawai, and E. Meyer, *Phys. Rev. B* **86**, 075407 (2012).

<sup>25</sup>G. Henkelman, B. P. Uberuaga, D. J. Harris, J. H. Harding, and N. L. Allan, *Phys. Rev. B* **72**, 115437 (2005).

<sup>26</sup>See Supplemental Material at <http://link.aps.org/supplemental/10.1103/PhysRevB.87.195437> for movies illustrating the transition between states  $E$  and  $A$  for the  $K^+$  terminated tip as observed in a molecular-dynamics simulation performed at 500 K (sup-movie1.avi). The total simulation time was 20 ps.

<sup>27</sup>See Supplemental Material at <http://link.aps.org/supplemental/10.1103/PhysRevB.87.195437> for movies illustrating ion displacements which accompany the approach and subsequent retraction of

a  $\langle 111 \rangle$ -directed KBr cubic model tip supporting an additional KBr dimer such that the initially protruding  $\text{Br}^-$  ion is above a  $\text{K}^+$  ion in the top layer of a KBr (001) slab. The movies were generated from snapshots taken at increments of 0.02 nm over nominal tip-sample distances between 1.07 and 0.13 nm and back, using the relaxation procedure described in Ref. 19. In the first movie (supmovie2.avi) the tip is approached up to a minimal distance of 1.3 Å to the surface. No jumps are observed. In the next movie (supmovie3.avi) the tip is approached up to a minimal distance of 1.1 Å to the surface, where a jump is clearly observed and a different configuration can be observed during retraction. The last movie (supmovie4) is viewed from the  $y$  direction, whereas the former two movies (2 and 3) are viewed from the  $x$  direction.

<sup>28</sup>The results shown in Fig. 2 were obtained in the direction from  $E$  to  $A$  with the exception of the path shown in gray above a surface  $\text{Br}^-$  for  $z = 4$  Å. For all other cases the barriers were assumed to be the same independent of the direction.

<sup>29</sup>P. V. Sushko, A. S. Foster, L. N. Kantorovich, and A. L. Shluger, *Appl. Surf. Sci.* **144–145**, 608 (1999).

<sup>30</sup>R. Oja and A. S. Foster, *Nanotechnology* **16**, S7 (2005).

<sup>31</sup>For a rotation angle of  $20^\circ$ , the dimer ions remain on the surface upon retraction if the tip is initially approached closer than 0.35 nm to the surface. The final state with the two additional ions transferred to the surface has an energy 310 meV lower than configuration  $E$ , because the dimer is now in a higher coordinated state on the surface compared to its location on a tip edge in configuration  $E$ .